

Octupole collectivity in the Sm isotopes

M. Babilon,^{1,2} N. V. Zamfir,^{1,3} D. Kusnezov,⁴ E. A. McCutchan,¹ and A. Zilges²

¹Wright Nuclear Structure Laboratory, Yale University, New Haven, Connecticut 06520-8124, USA

²Institut für Kernphysik, Technische Universität Darmstadt, Schlossgartenstrasse 9, D-64289 Darmstadt, Germany

³National Institute for Physics and Nuclear Engineering, Bucharest-Magurele, Romania

⁴Sloane Physics Laboratory, Yale University, New Haven, Connecticut 06520-8120, USA

(Received 3 March 2005; published 8 December 2005)

Microscopic models suggest the occurrence of strong octupole correlations in nuclei with $N \approx 88$. To examine the signatures of octupole correlations in this region, the *spdf* interacting boson approximation model is applied to Sm isotopes with $N = 86$ –92. The effects of including multiple negative-parity bosons in this basis are compared with more standard one negative-parity boson calculations and are analyzed in terms of signatures for strong octupole correlations. It is found that multiple negative-parity bosons are needed to describe properties at medium spin. Bands with strong octupole correlations (multiple negative-parity bosons) become yrast at medium spin in ^{148,150}Sm. This region shares some similarities with the light actinides, where strong octupole correlations were also found at medium spin.

DOI: [10.1103/PhysRevC.72.064302](https://doi.org/10.1103/PhysRevC.72.064302)

PACS number(s): 21.60.Fw, 21.10.Re, 27.60.+j, 27.70.+q

I. INTRODUCTION

Much recent work has been devoted to the study of octupole deformation. However, the answer to the question of whether nuclei with octupole deformation exist and, if so, where they are located in the nuclear landscape, has remained elusive. So far, no definitive experimental signatures have been established. Many different models have been considered (for a review see, e.g. [1]), but none have provided a complete picture of octupole deformation. Recently, however, a description of nuclei in the actinides with a simple *spdf* Hamiltonian [2–4] in the framework of the interacting boson approximation (IBA) model [5] has been given in [6], in which some signs of strong octupole correlations at medium spins were observed. This paper gives a description of nuclei in the rare-earth region, where strong octupole correlations may also occur.

In a microscopic picture, the origin of octupole collectivity can be explained by the interplay of the unique parity orbit in each major shell and a common parity orbit that differ by angular momentum and total spin $\Delta l = \Delta j = 3$. Octupole correlations are strongest when the Fermi surface lies between those orbits and the octupole operator has a maximum contribution. The microscopic point of view [7] predicts the occurrence of strong octupole correlations at neutron and proton numbers $N, Z = 56$ and 88. Cottle [8] suggests that $N, Z = 64$ and 88 should be considered because the energies of the first 3^- states are expected to be at a minimum for the nuclei that are most octupole deformed. These predictions, combined with the fact that a wealth of experimental information is known about many excited negative-parity bands in the Sm isotopes, prompted us to investigate systematically this region within the framework of the IBA model with multiple negative-parity bosons. Previous IBA calculations in this region [9–13] studied the low-lying negative-parity states considering only one *f* boson that would correspond in the geometrical picture to octupole vibrations. A systematic study of [12] showed that the *sdf* Hamiltonian can successfully describe the octupole vibrational bands in quadrupole-deformed nuclei in this region.

The expression “strong octupole correlations” used throughout this paper implies that the content of *f* bosons in the wave functions is greater than one.

The aim of this paper is to study to what extent strong octupole correlations are present in the negative-parity bands, especially in highly excited states, in the Sm isotopes. We achieve this by enlarging the model space to more than one negative-parity boson. Introducing also *p* bosons will establish the position of these isotopes relative to the rotational dynamical symmetry inherently generated by the corresponding group structure of U(16). In addition, the presence of the *p* boson in the calculations will allow the use of a simple one-body *E1* operator that can give information about the dipole degree of freedom present in the highly excited states in these nuclei.

In Sec. II, we introduce the Hamiltonian for this study. Although such a form has been applied to the actinides, this is, to our knowledge, the first such study in the rare earths. It provides the ability to explore issues of octupole deformation in ground and excited states. In Sec. III, we present results of IBA calculations in which one negative parity boson was coupled to positive-parity states, whereas in Sec. IV we discuss the effects of coupling multiple negative-parity bosons to positive-parity states. Finally, hints of strong octupole correlations of an excited $K^\pi = 0^+$ band in ¹⁵²Sm are presented in Sec. V.

II. MODEL HAMILTONIAN

As a starting point for the calculations, we first identify the Hamiltonian for the positive-parity states. We use the Hamiltonian of Scholten, Iachello, and Arima [9], which has successfully described various observables in even-even Sm isotopes with $A = 148$ –154 covering the evolution from spherical to quadrupole-deformed nuclei. It can be written in a simplified form:

$$H_{sd} = \epsilon_d \hat{n}_d + \kappa \hat{Q}_{sd}^{(2)} \cdot \hat{Q}_{sd}^{(2)}. \quad (1)$$

This Hamiltonian contains only the d boson number operator \hat{n}_d and a quadrupole-quadrupole interaction term with $\hat{Q}_{sd}^{(2)} = [s^\dagger \tilde{d} + d^\dagger \tilde{s}]^{(2)} - \frac{\sqrt{7}}{2} [d^\dagger \tilde{d}]^{(2)}$. We do not include the $\hat{L} \cdot \hat{L}$ term. Although it can be used to improve the agreement of the predicted energy eigenvalues with experiment by modifying the moment of inertia while leaving the eigenfunctions intact, it introduces an additional parameter.

In the next step, we realize the full spectrum of the Hamiltonian, which includes negative-parity states, by taking H_{sd} and replacing the operators with their respective extensions in the larger boson space of s ($l = 0$), p ($l = 1$), d ($l = 2$), and f ($l = 3$) bosons. The resulting Hamiltonian is

$$H_{spdf} = \epsilon_p \hat{n}_p + \epsilon_d \hat{n}_d + \epsilon_f \hat{n}_f + \kappa \hat{Q}_{spdf}^{(2)} \cdot \hat{Q}_{spdf}^{(2)}, \quad (2)$$

$$\hat{Q}_{spdf}^{(2)} = [s^\dagger \tilde{d} + d^\dagger \tilde{s}]^{(2)} - \frac{\sqrt{7}}{2} [d^\dagger \tilde{d}]^{(2)} + \frac{3\sqrt{7}}{5} [p^\dagger \tilde{f} + f^\dagger \tilde{p}]^{(2)} - \frac{9\sqrt{3}}{10} [p^\dagger \tilde{p}]^{(2)} - \frac{3\sqrt{42}}{10} [f^\dagger \tilde{f}]^{(2)}. \quad (3)$$

This has the advantage of preserving the structure of the positive-parity states and using the predicted quadrupole strength parameter κ to determine the structure of the negative-parity states. The new quadrupole operator \hat{Q}_{spdf} is now the generator of the $SU_{spdf}(3)$ dynamical symmetry that exists in the larger $spdf$ boson space [3,4]. Note that it includes the \hat{Q}_{sd} operator in it as well. Consequently, the only freedom in describing the negative parity states lies in the p and f boson vibrational energies ϵ_p and ϵ_f . However, these are defined largely by the experimental locations of the lowest 1^- and 3^- states.

For $E1$ and $E2$ transitions, we need to define appropriate one-body transition operators. The quadrupole operator \hat{Q}_{spdf} provides a natural choice for the quadrupole transition operator $\hat{T}(E2) = e_2 \hat{Q}_{spdf}$. This leaves the effective charge e_2 as the only degree of freedom. For $E1$ transitions there is no natural operator in the $spdf$ algebra. Consequently, a linear combination of the three allowed one-body interactions was taken:

$$\hat{T}(E1) = e_1 \{ \chi_{sp} [s^\dagger \tilde{p} + p^\dagger \tilde{s}]^{(1)} + [p^\dagger \tilde{d} + d^\dagger \tilde{p}]^{(1)} + \chi_{df} [d^\dagger \tilde{f} + f^\dagger \tilde{d}]^{(1)} \}. \quad (4)$$

The effective charge e_1 and $\chi_{sp,df}$ are unknown parameters and will be required to vary smoothly in the systematics we study in this region.

The Hamiltonian is typically diagonalized in a Hilbert space with a total number of bosons $N_B = n_s + n_d + n_p + n_f$. We have found that when we are interested in the low-lying states of Eq. (2) with typical parameters [6], diagonalization in the subspace with $n_p + n_f = 1$ is sufficient. That is, low-lying negative parity states are often consistent with a single negative-parity boson coupled to the positive-parity states. The effects of more complex configurations with $n_p + n_f > 1$ are to introduce more deformed octupole bands (two or more negative-parity bosons) at higher excitation, but can also lead to (small) admixtures into the yrast bands and low-lying excited states. The latter are characterized by nonzero expectation values n_p and n_f in the states. To simplify the analysis, we first explore the $n_p + n_f \leq 1$ states, followed

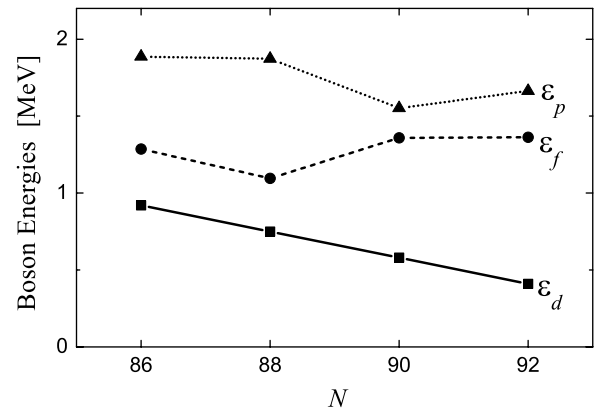


FIG. 1. The energies for the three types of bosons, p , d , and f , exhibit a smooth behavior across the Sm isotopes with masses ranging from $A = 148$ to $A = 154$.

by the effects of more deformed configurations in the spectra ($n_p + n_f > 1$).

III. POSITIVE-PARITY STATES COUPLED TO ONE NEGATIVE-PARITY BOSON

To lowest order, the spectrum of the Hamiltonian is obtained by the coupling of a single p or f boson to the positive-parity states. For the Sm nuclei we examine, the boson number is $N_B = N_\pi + N_\nu$, where N_π (N_ν) is given by half the number of valence protons (neutrons) relative to shell closures at 50 (82). The parameters used previously for the study of the positive-parity states, ϵ_d and κ , are adopted [9]. In particular, the strength for the quadrupole-quadrupole interaction is kept constant at $\kappa = -19.5$ keV [9] in all calculations. We obtain the p and f boson energies, ϵ_p and ϵ_f , by considering the first few excited states in the negative-parity bands. Figure 1 shows the boson energies ϵ_p , ϵ_d , and ϵ_f for the $^{148-154}\text{Sm}$ isotopes.

A comparison of the lowest-yrast-energy levels in the $^{148-154}\text{Sm}$ isotopes with $N = 86-92$ are displayed in Fig. 2.

The evolution of structure from vibrational type, with relatively large 2_1^+ energy and $R_{4/2}$ close to 2.0 ($R_{4/2} = 2.14$ in $^{148}\text{Sm}_{86}$), to rotational type, with small 2_1^+ energy and $R_{4/2}$ close to 3.33 ($R_{4/2} = 3.25$ in $^{154}\text{Sm}_{92}$), is well reproduced, as

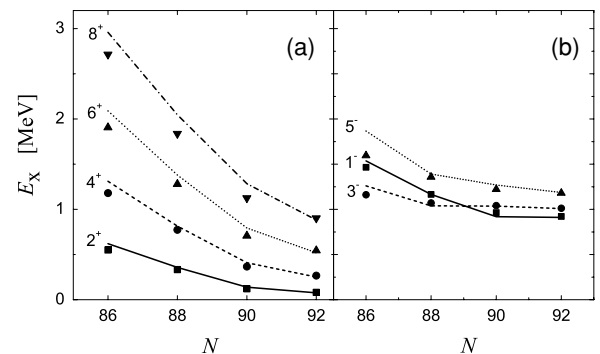


FIG. 2. Comparison of experimental values [14–17] for energies of the first $K^\pi = 0^\pm$ states (symbols) in $^{148-154}\text{Sm}$ with the calculated energies in our Hamiltonian (curves).

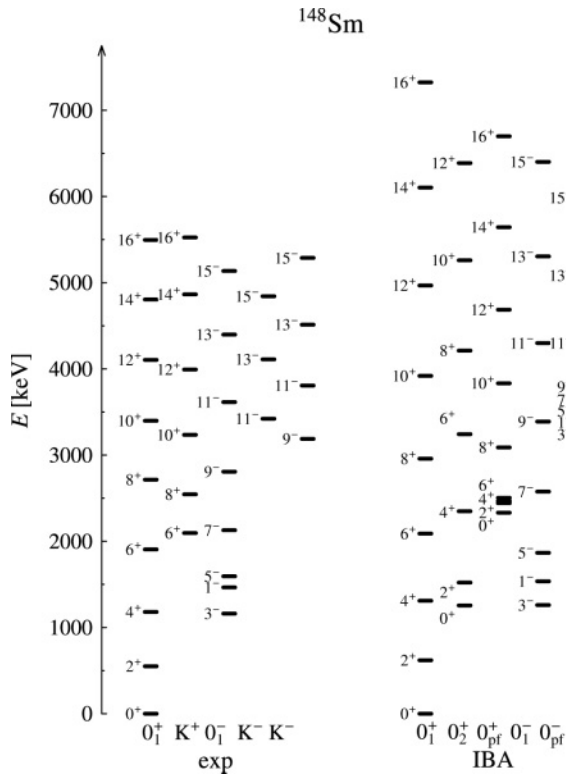


FIG. 3. Experimentally observed (left) and theoretically calculated (right) low-lying states in ^{148}Sm . Calculated bands with a higher content of negative-parity bosons are labeled with “ pf .”

can be seen in Fig. 2(a). This trend can be described in the IBA by a decrease in the strength of the vibrational component of the Hamiltonian ϵ_d (see Fig. 1) and an increase in the rotational part that, when κ is kept constant, is growing only because of the larger number of bosons. The variation in energies of the negative-parity states [Fig. 2(b)] is less dramatic in this mass region, as can be seen in the nearly constant values of ϵ_p and ϵ_f shown in Fig. 1. This behavior is distinct from that observed in the actinides [6,18], in which both ϵ_p and ϵ_f have a minimum for $N_B \approx 8$ and increase afterwards. For a spherical vibrational nucleus, the first 1^- state results from the coupling of an octupole (3^-) and a quadrupole (2^+) boson, and in the harmonic limit, the 1^- state, which is a member of a quintuplet $3^- \otimes 2^+ = 1^-$ to 5^- , should be located at the sum of the energies of the octupole and quadrupole bosons. When a transition to quadrupole-deformed shapes occurs, a bandlike structure with a sequence of spins $1^-, 3^-, 5^-, \dots$, is expected. This evolution is also well reproduced by the model.

Figures 3–6 show more detailed comparisons of experimental energy levels (left-hand side) with IBA results (right-hand side). For reference, calculations with up to three p, f bosons are included (these bands are labeled “ pf ” and are discussed in the next section). The levels are shown in a quasi band structure, as proposed in Ref. [19]. The quasi bands are labeled according to the quasi quantum number K (the projection of the total angular momentum on the symmetry axis is a good quantum number only in axially symmetric, strongly quadrupole-deformed nuclei). In ^{148}Sm , all bands adopted

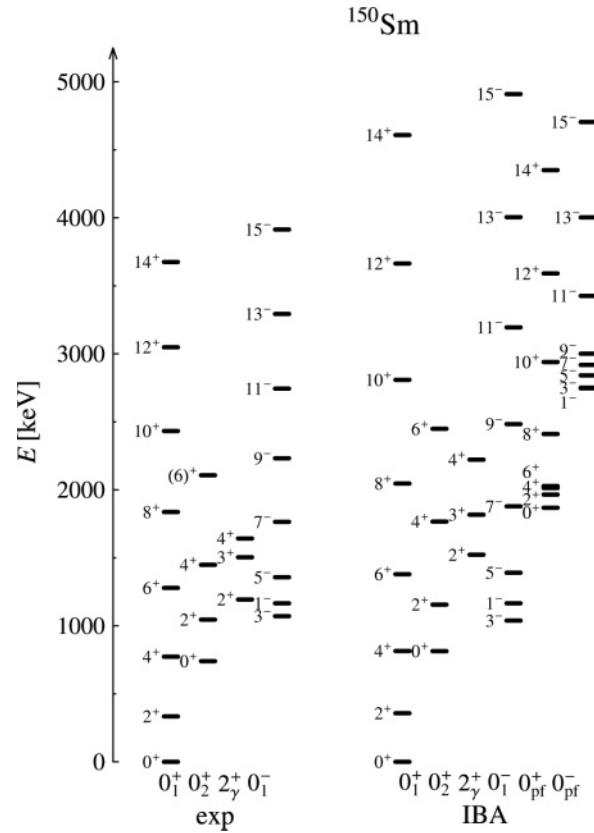


FIG. 4. Same as Fig. 3, but for ^{150}Sm .

in [14] are displayed, despite the fact that two of them, based on an 8^+ state at 2246 keV and an 11^- level at 3422 keV, possibly have a single-particle character [20]. Furthermore, because for nonyrast bands neither the collective character nor the bandheads have been assigned clearly, the level sequences are denoted by K^\pm . They are included in the comparison because of the possibility that these sequences are part of the $K_i^\pi = 0_2^+$ and $K_i^\pi = 0_2^-$ bands and their low-spin part is not experimentally known.

The agreement in Figs. 3–6 between the experimental data and theoretical calculations is good. The bandheads are very well described, with the exception of the 2_2^+ band, which is off by about 200 keV. The moments of inertia are underestimated in all cases, except for ^{154}Sm .

A proposed signature for octupole deformation is the occurrence of an alternating parity band [21]. The $K_i^\pi = 0_1^+$ and 0_1^- quasi bands appear to behave as alternating parity-bands at medium spins. To better understand this, we use a sensitive quantity, the signature-splitting index $S(J)$ [22], which describes the normalized position of a negative-parity level J^- relative to the positive-parity ones with spin and parity $(J \pm 1)^+$:

$$S(J) = \frac{[E_{J+1} - E_J] - [E_J - E_{J-1}]}{E_{2_1^+}}. \quad (5)$$

An alternating parity band would provide an equal spacing of the levels, so that $S(J)$ would be approximately zero. Decreasing experimental signature splittings with increasing

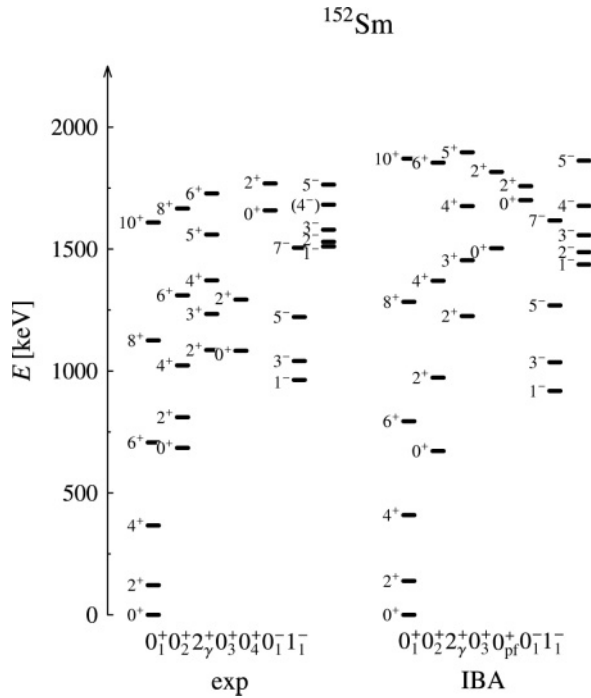


FIG. 5. Same as Fig. 3, but for ^{152}Sm .

spin are observed for $^{148-154}\text{Sm}$. At a certain spin, J_{crit} , the signature splitting approaches zero [$S(J) \rightarrow 0$]. As shown in Figs. 7 (top) and 8, J_{crit} increases with mass ($J_{\text{crit}} \approx 5$ for $A = 148$, ≈ 11 for $A = 150$, and >13 for $A = 152, 154$). The IBA calculations reproduce the gross behavior. Experimental values of $S(J)$ in $^{148,150}\text{Sm}$ (Fig. 7, top) exhibit a change in the trend after the critical value, suggesting a change in structure in the involved bands. Calculations with one negative-parity

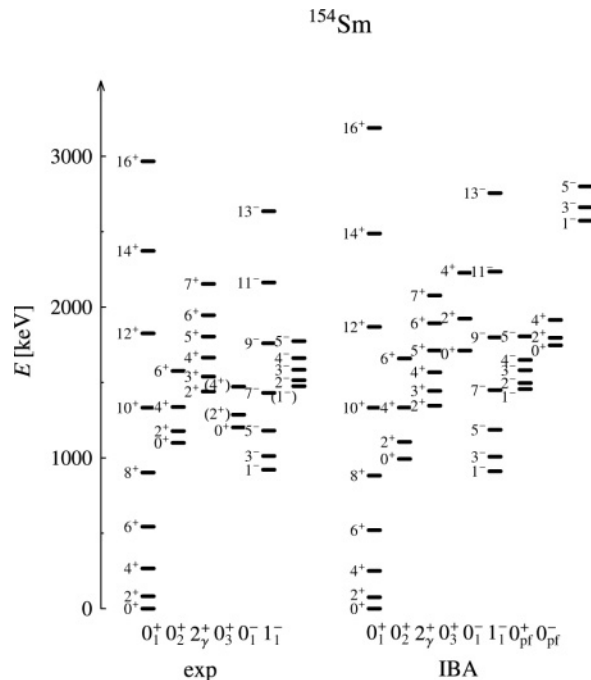


FIG. 6. Same as Fig. 3, but for ^{154}Sm .

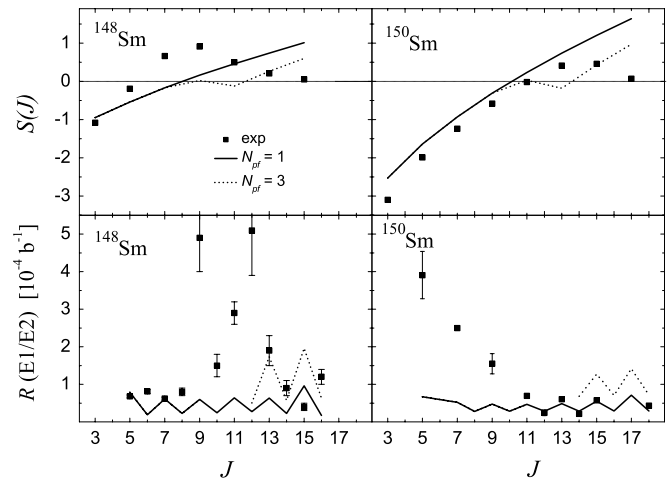


FIG. 7. (Top) Experimental signature-splitting index $S(J)$ (symbols) for ^{148}Sm (left) and ^{150}Sm (right) compared with theory with $N_{pf} = 1$ and 3 (lines). (Bottom) Ratio of electric dipole and quadrupole strengths for the same nuclei. The effective charges, $e_1 = 0.010 e b^{1/2}$ and $e_2 = 0.13 e b$, are the same for both isotopes.

boson (solid lines in upper part of Fig. 7) are unable to reproduce this change in behavior in the signature-splitting index. The onset of strong octupole correlations may affect the bands and explain the changes, as is discussed below. In contrast, the signature-splitting indices for ^{152}Sm and ^{154}Sm (Fig. 8) give no hint of strong octupole correlations, as $S(J)$ does not approach 0 (no alternating parity band) in the available data.

Electromagnetic transition rates are also a useful tool for testing the wave functions. The electric quadrupole strengths among the positive-parity states were studied by Scholten *et al.* [9]. We present in Fig. 9 the comparison of the experimental absolute $B(E2)$ strengths between yrast states in all even-even Sm isotopes with the IBA results. Agreement is obtained by use of a unique effective charge ($e_2 = 0.13 e b$ [9])

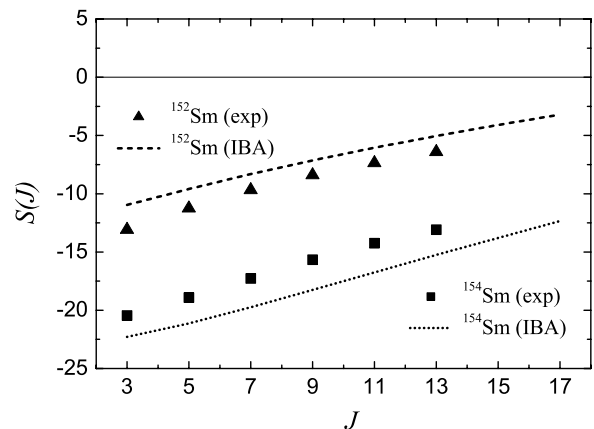


FIG. 8. Experimental signature-splitting index $S(J)$ (symbols) for ^{152}Sm and ^{154}Sm compared with theory with $N_{pf} = 1$ (lines).

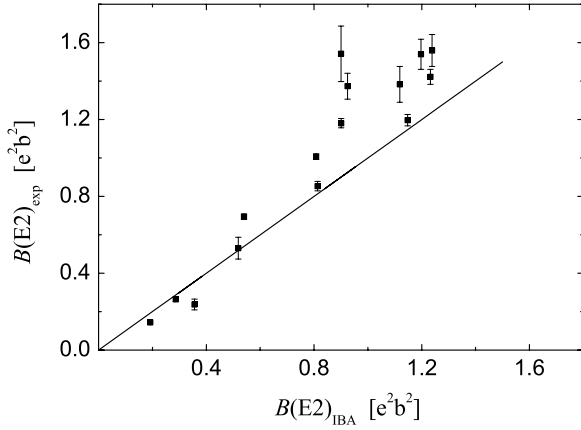


FIG. 9. Comparison between experimental $B(E2)$ strengths from the 0_1^+ bands in $^{148-154}\text{Sm}$ and theory, with a constant effective charge $e_2 = 0.13 e b$ [9].

for all Sm isotopes. The absolute $B(E2)$ values among the negative-parity states are not experimentally known, but sets of $B(E1)/B(E2)$ ratios were measured in the Sm isotopes, as discussed below. First we discuss the $B(E1)$ strengths. The ratio of electric dipole transition strengths,

$$R(E1) = \frac{B[E1; J^- \rightarrow (J+1)^+]}{B[E1; J^- \rightarrow (J-1)^+]}, \quad (6)$$

is dependent on only the internal parameters and not on the effective charge. In Fig. 10 a comparison between experimental dipole strength ratios in $^{150,152,154}\text{Sm}$ and IBA calculations is shown; the parameters of Fig. 11 are used. Data for each of these nuclei show a decrease in the ratio of electric dipole transition strength for increasing spin, starting from $R(E1) \approx 2$ for spin $J = 1$ and $R(E1) \approx 1$ for $J > 1$. This trend is well reproduced by the calculations with a variation of the strength parameters of the matrix elements in the $\hat{T}(E1)$ operator only in a small range from -0.25 to -0.35 . In ^{148}Sm , excited members of the $K_i^\pi = 0_1^+$ band are higher in energy relative to $K_i^\pi = 0_1^-$ bands, and therefore $R(E1)$ exists for only the 1_1^- state [$R(E1)_{\text{exp}} = 2.13(46)$] and is reasonably reproduced by the IBA calculation [$R(E1)_{\text{IBA}} = 2.82$].

We obtain the effective charge e_1 for electric dipole transition strengths by taking into account all absolute strengths given in Refs. [14–16,23]. A value of $e_1 = 0.010 e b^{1/2}$ is used for all Sm isotopes. Figure 12 shows a comparison between all experimentally known absolute $E1$ strengths from 1^- to 0^+ states as well as 3^- to 2^+ states and theory. The $B(E1; 3^- \rightarrow 2^+)$ transition also shows very good agreement between

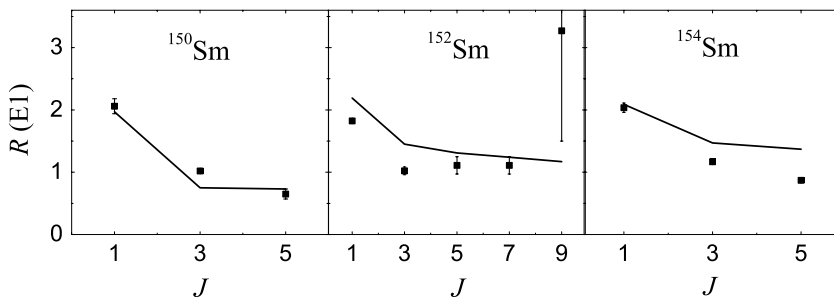


FIG. 10. Comparison of experimental (points) and predicted (lines) ratios of electric dipole strengths for $^{150,152,154}\text{Sm}$.

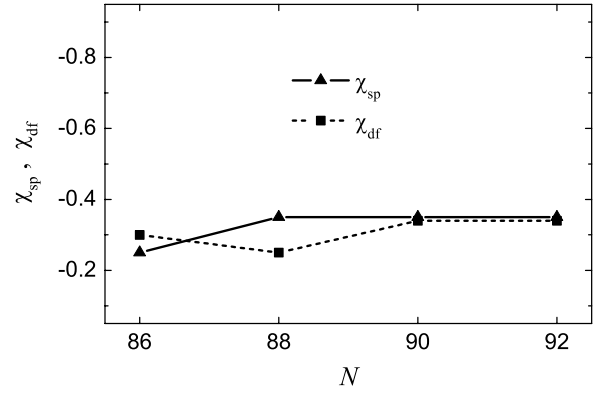


FIG. 11. Parameters of the $\hat{T}(E1)$ operator vary in only a small range from -0.25 to -0.35 for $^{148-154}\text{Sm}$.

experiments and theory. For $B(E1; 1^- \rightarrow 0^+)$ transitions, the calculations slightly overestimate the data, but the trend is well described.

With both absolute electric dipole and quadrupole transition strengths well defined, another value, the ratio of reduced transition strengths from an energy level with spin J , can be obtained that also provides a very sensitive test of the wave functions:

$$R(E1/E2) = \frac{B(E1; J \rightarrow J-1)}{B(E2; J \rightarrow J-2)}. \quad (7)$$

Data are available in $^{148,150}\text{Sm}$ on branchings from negative-parity odd J states as well as interband/intraband transitions from positive-parity even J levels. In the lower part of Fig. 7, the ratios $R(E1/E2)$ from the $N_{pf} = 1$ calculations (solid lines) are compared with the experimental data. For ^{148}Sm , the fluctuations in the spin region $J = 9-12$ could not be reproduced, but the mean value for the experimentally obtained $R(E1/E2)$ is in agreement with the calculation (solid line). In ^{150}Sm , for higher spins, good agreement is obtained; for lower spins, deviations of about a factor of 4 can be seen. One should note that the experimental data points, which diverge from the model, either have large uncertainties or the uncertainties are not given. More precise data on ^{150}Sm could clarify this situation.

IV. POSITIVE-PARITY STATES COUPLED TO MULTIPLE NEGATIVE-PARITY BOSONS

In the signature-splitting diagrams, Figs. 7 and 8, changes in the structures of the bands (0_1^+ and 0_1^- bands for $^{148,150}\text{Sm}$)

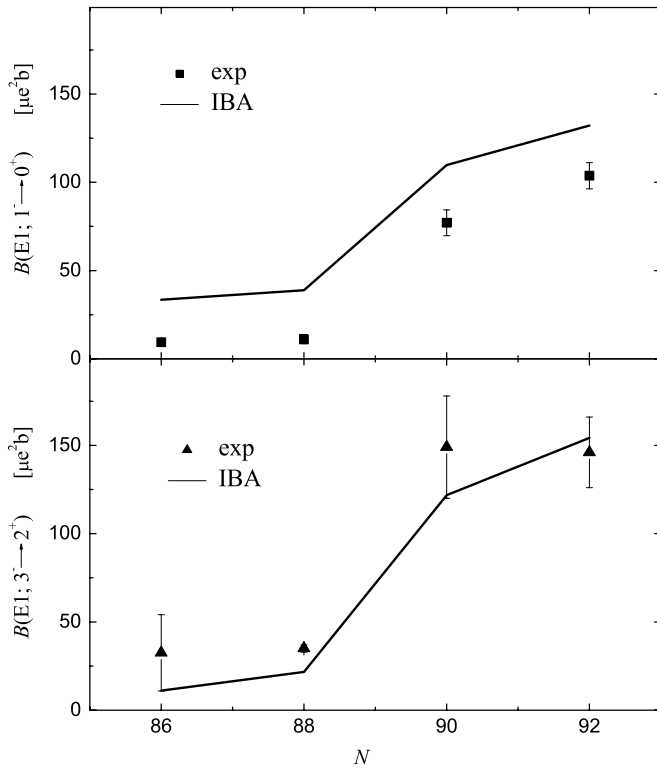


FIG. 12. Evolution of absolute $B(E1)$ strengths in $^{148-154}\text{Sm}$ for $1^- \rightarrow 0^+$ and $3^- \rightarrow 2^+$ transitions. The effective charge $e_1 = 0.010 e b^{1/2}$ is kept constant for all Sm isotopes.

are observed at medium spin. We investigated these to see whether they can be interpreted as signatures of stronger octupole correlations. We do this by extending the basis to include multiple negative-parity bosons. Because of limitations in computer power, we had to restrict the number of negative-parity bosons to three ($N_{pf} = 3$). This extension of the basis should lead to additional octupole-deformed bands, i.e., bands with a higher content of p and f bosons ($n_p + n_f > 1$). In addition to the bands described by the $N_{pf} = 1$ calculations, additional bands are obtained with a content of two p , f bosons for positive-parity and three p , f bosons for negative-parity bands (labeled as “ pf ”). The new positive-parity ($N_{pf} = 2$) pf bands appear to be the second excited 0^+ ($K_i^\pi = 0_3^+$) bands for $^{148,150}\text{Sm}$ and the third ($K_i^\pi = 0_4^+$) for $^{152,154}\text{Sm}$, whereas new negative-parity bands ($N_{pf} = 3$) are higher in energy than the first three or four $K^\pi = 0^-$ bands with $n_p + n_f = 1$. These new bands become yrast at $J^\pi = 10^+/11^-$ in ^{148}Sm and $J^\pi = 12^+/13^-$ in ^{150}Sm , respectively. In contrast, the bands in $^{152,154}\text{Sm}$ with a higher content of p , f bosons are highly excited and do not become yrast.

There are two effects in Figs. 7 and 8 that we would like to interpret in terms of octupole-dipole collectivity. The first is the change in character of $S(J)$ near zero in $^{148-150}\text{Sm}$ and the second is the relative magnitude of $S(J)$ between $^{148-150}\text{Sm}$ and $^{152-154}\text{Sm}$.

We examined the changes observed in the behavior of $S(J)$ near $S \approx 0$ in terms of band crossings. Including the new yrast

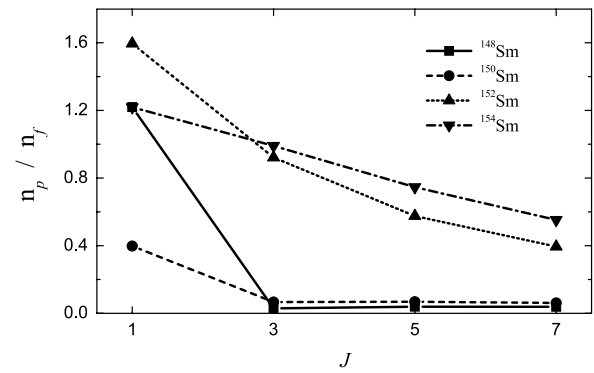


FIG. 13. Ratio of expectation values for the number of p to the number of f bosons in the low-lying negative-parity states. The octupole nature in $^{148-150}\text{Sm}$ is evident by the lack of p boson content. These are also the nuclei that exhibit alternating parity bands. The similarity of p and f boson content in $^{152-154}\text{Sm}$ states is a reflection of the Hamiltonian nearing the (SU_{spdf}) rotational limit in the full boson space. These near-rotational nuclei do not exhibit the alternating parity bands.

states, discussed above, the signature-splitting indices $S(J)$ (dashed lines in upper part of Fig. 7) for the 0_1^+ and 0_1^- bands show obvious hints of the experimentally suggested change in structure. Although the turnover seems to occur at roughly the same spin, this change does not follow the experimental trend for higher spins, and the new theoretical $S(J)$ values continue to increase toward larger positive values. Although suggestive, the crossing of a band with stronger octupole content does not capture the entire effect.

The second interesting aspect is the relative magnitudes of $S(J)$ between $^{148-150}\text{Sm}$ and $^{152-154}\text{Sm}$. This seems to be well captured by our simple Hamiltonian. Consider the expectation values for the number of p and f bosons in the low-lying negative-parity yrast states, as shown in Fig. 13. In $^{148,150}\text{Sm}$, for states with spin $J \geq 3$, the f boson dominates in the ratio, which reflects the mostly octupole nature of these states. We also note that in these two nuclei the signature splitting approaches zero. In $^{152,154}\text{Sm}$, the p and f contents are comparable and $S(J)$ is very large. This fact suggests that the appearance of the alternating parity bands [$S(J) \rightarrow 0$] is closely related to the exclusive octupole character (f boson) of the negative-parity states.

In addition, in $^{152,154}\text{Sm}$, the energies of p and f boson become similar ($\epsilon_p \approx \epsilon_f$; see Fig. 1). The significance of this near degeneracy is the proximity to the rotational limit of Eq. (2) [18,24]. When $\epsilon_p = \epsilon_f$ and $\epsilon_d = 0$ in our Hamiltonian, we have a $\text{SU}_{spdf}(3)$ dynamical symmetry. Interestingly, this rotational limit is not consistent with the appearance of the alternating parity bands [or $S(J) \approx 0$]. These bands appear for specific values of energies of only the negative-parity bosons, namely, $\epsilon_p = \epsilon_f = \kappa(2N_B + 4)$ [18]. As the neutron number develops, the nuclei tend to a rotational limit but do not alternate parity bands. In the transition region, where octupoles play a more dominant role, we find these bands appearing at relatively low spin.

One property of the $N_{pf} > 1$ configurations included in the Hamiltonian equation (2) is that states with larger pf content

TABLE I. Absolute $B(E1)$ and $B(E2)$ strengths from the 0^+ state at 1659 keV in ^{152}Sm compared with the corresponding predictions for the 0^+_{pf} state.

Absolute strength	Exp [15]	IBA
$B(E1; 0^+_4 \rightarrow 1^-_1)$	$1.5(11) \mu e^2 \text{ b}^2$	$618 \mu e^2 \text{ b}^2$
$B(E2; 0^+_4 \rightarrow 2^+_2)$	$0.39(29) \text{ me}^2 \text{ b}^2$	$0.94 \text{ me}^2 \text{ b}^2$
$B(E2; 0^+_4 \rightarrow 2^+_1)$	$9.6(77) \mu e^2 \text{ b}^2$	$7.52 \mu e^2 \text{ b}^2$

do not interact with states with lower content. Wave functions of the members of the $n_{pf} = 0$ and $n_{pf} = 2$ bands for positive parities or $n_{pf} = 1$ and $n_{pf} = 3$ bands for negative parities are not connected through the one-body transition operators. Consequently, the measurement of transitions between states near $S(J) \approx 0$ might shed light on the observed behavior. It is possible to add an interaction term, H_{int} , that connects the respective bands, such as

$$H_{\text{int}} = \alpha' ([d^\dagger d^\dagger]^{(4)} \cdot [\tilde{f} \tilde{f}]^{(4)} + \text{Hc}). \quad (8)$$

However, existing data fix the strength of this term only at $\alpha' = 40$ keV, but it does not have any predictive value. Such a mixing term causes only slight changes to the above-discussed properties of energies and transition strengths, while breaking the symmetry sufficiently to enable transitions between the two types of bands. Further extensions of the Hamiltonian with additional mixing terms also did not change considerably the content of negative-parity bosons in the wave functions of the ground state and of excited states. Moreover, additional data are needed to clarify the band-crossing interpretation of $S(J)$.

V. EXCITED $K^\pi = 0^+_{pf}$ BAND IN ^{152}SM

It has been mentioned that the inclusion of more negative-parity bosons in the basis produces additional octupole-deformed bands with a higher content of p and f bosons and that in $^{148,150}\text{Sm}$ these new bands become yrast at higher spins. In ^{152}Sm , our Hamiltonian predicts that the 0^+_4 (1701-keV) and the 2^+_4 (1758-keV) states are members of a band higher in energy with a strong octupole correlation that may correspond to the experimental 0^+ state at $E_x = 1659$ keV and the 2^+ level at $E_x = 1769$ keV.

The reduced strength for the quadrupole transition between these states is predicted to be $B(E2; 2^+_4 \rightarrow 0^+_4) = 202 \text{ W.u.}$ (Weisskopf units), and the relative branching from the 2^+_4 to the 0^+_4 and 0^+_1 is calculated to be 10^5 . In the existing measurement, despite the high statistics [25], the 2^+ (1769-keV) \rightarrow 0^+ (1659-keV), 110-keV transition was not seen. Only an upper limit for this intensity can be given as 10^{-4} relative to the intensity of the 2^- (1530-keV) \rightarrow 1^- (963-keV), 566-keV transition. This intensity limit, corresponding to a relatively large transition strength, agrees with the IBA calculation.

The experimental 0^+ state (1659 keV) and the 2^+ level (1769 keV) decay by means of several transitions.

TABLE II. Ratios of reduced electric dipole and quadrupole strengths from the 2^+_4 state in ^{152}Sm are compared to experimental transition strengths from the 2^+ at 1769 keV. Very good agreement was obtained for pure dipole or quadrupole ratios.

Strength ratio	Exp [15]	IBA
$\frac{B(E1; 2^+_4 \rightarrow 3^-_1)}{B(E1; 2^+_4 \rightarrow 1^-_1)}$	1.24(14)	4.27
$\frac{B(E2; 2^+_4 \rightarrow 0^+_1)}{B(E2; 2^+_4 \rightarrow 2^+_1)}$	1.06(12)	1.31
$\frac{B(E2; 2^+_4 \rightarrow 2^+_2)}{B(E2; 2^+_4 \rightarrow 2^+_1)}$	51.7(78)	55.6

However, absolute $B(E1)$ and $B(E2)$ strengths are known for only the 0^+ state. The experimental electric quadrupole transition strengths [15] presented in Table I are in good agreement with calculated values, but the IBA overestimates the $B(E1)$ strength by about a factor of 400. For the 2^+ level at 1769 keV, only branching ratios [15] are known, and a comparison with the IBA calculation is given in Table II.

The good agreement between experimental and calculated strength ratios, despite the deviation for absolute $B(E1)$ strengths, leads to the conclusion that the excited 0^+ band, with its bandhead at 1701 keV, possibly shows strong octupole correlations.

VI. CONCLUSIONS

IBA calculations made with a $spdf$ Hamiltonian reproduce the majority of data related to the low-lying positive- and negative-parity states in $^{148-154}\text{Sm}$. The comparison reveals the strong octupole correlation character, i.e., multiple negative-parity bosons in the wave functions of states of some excited bands that become yrast at medium spin ($J \approx 10$) in $^{148,150}\text{Sm}$. No such effect is present in $^{152,154}\text{Sm}$. However, these two nuclei present another interesting feature, namely some characteristics related to the $\text{SU}(3)_{spdf}$ dynamical symmetry limit. As indicated in Ref. [18], the appearance of the alternating parity bands in this dynamical symmetry limit is accidental for only specific values of the Hamiltonian parameters. Indeed, the corresponding bands in $^{152,154}\text{Sm}$ exhibit a strong dipole/octupole nature, but they do not form an alternating parity band (the signature splitting is not approaching zero). In addition, an excited band in ^{152}Sm with the bandhead at 1701 keV shows strong octupole correlations. To present reliable predictions regarding octupole behavior, additional experiments have to be performed on neighboring nuclei that will allow extending the present calculations.

ACKNOWLEDGMENTS

We gratefully acknowledge valuable discussions with F. Iachello and R. F. Casten as well as L. F. dos Santos for her preceding work on Sm isotopes. This work is supported by the U.S. Department of Energy under grant no. DE-FG02-91ER-40609 and by Deutsche Forschungsgemeinschaft grant nos. SFB 634 and Zi 510/2-2.

- [1] P. A. Butler and W. Nazarewicz, *Rev. Mod. Phys.* **68**, 349 (1996).
- [2] D. F. Kusnezov and F. Iachello, *Phys. Lett.* **B209**, 420 (1988).
- [3] D. F. Kusnezov, Ph.D. thesis, Princeton University (1988).
- [4] D. Kusnezov, *J. Phys. A* **22**, 4271 (1989).
- [5] F. Iachello and A. Arima, *The Interacting Boson Model* (Cambridge University Press, Cambridge, 1987).
- [6] N. V. Zamfir and D. Kusnezov, *Phys. Rev. C* **67**, 014305 (2003).
- [7] W. Nazarewicz, P. Olanders, I. Ragnarsson, J. Dudek, G. A. Leander, P. Möller, and E. Ruchowska, *Nucl. Phys.* **429**, 269 (1984).
- [8] P. D. Cottle, *Phys. Rev. C* **42**, 1264 (1990).
- [9] O. Scholten, F. Iachello, and A. Arima, *Ann. Phys. (NY)* **115**, 325 (1978).
- [10] Z. Sujkowski, D. Chmielewska, M. J. A. de Voigt, J. F. W. Jansen, and O. Scholten, *Nucl. Phys.* **A291**, 365 (1977).
- [11] J. Konijn, J. B. R. Berkhout, W. H. A. Hesselink, J. J. van Ruijven, P. van Nes, H. Verheul, F. W. N. de Boer, C. A. Fields, E. Sugarbaker, P. M. Walker *et al.*, *Nucl. Phys.* **373**, 397 (1982).
- [12] A. F. Barfield, B. R. Barrett, J. L. Wood, and O. Scholten, *Ann. Phys. (NY)* **182**, 344 (1988).
- [13] N. V. Zamfir and P. von Brentano, *Phys. Lett.* **B289**, 245 (1992).
- [14] M. R. Bhat, *Nucl. Data Sheets* **89**, 797 (2000).
- [15] A. Artna-Cohen, *Nucl. Data Sheets* **79**, 1 (1996).
- [16] C. W. Reich and R. G. Helmer, *Nucl. Data Sheets* **85**, 171 (1998).
- [17] E. Dermateosian and J. K. Tuli, *Nucl. Data Sheets* **75**, 827 (1995).
- [18] N. V. Zamfir and D. Kusnezov, *Phys. Rev. C* **63**, 054306 (2001).
- [19] M. Sakai, *At. Data Nucl. Data Tables* **31**, 399 (1984).
- [20] W. Urban, R. M. Lieder, J. C. Bacelar, P. P. Singh, D. Alber, D. Balabanski, W. Gast, H. Grawe, G. Hebbinghaus, J. R. Jongman *et al.*, *Phys. Lett.* **B258**, 293 (1991).
- [21] G. A. Leander, R. K. Sheline, P. Möller, P. Olanders, I. Ragnarsson, and A. J. Sierk, *Nucl. Phys.* **388**, 452 (1982).
- [22] N. V. Zamfir, P. von Brentano, and R. F. Casten, *Phys. Rev. C* **49**, R605 (1994).
- [23] A. Jungclaus, H. G. Börner, J. Jolie, S. Ulbig, R. F. Casten, N. V. Zamfir, P. von Brentano, and K. P. Lieb, *Phys. Rev. C* **47**, 1020 (1993).
- [24] D. Kusnezov, *J. Phys. A: Math. Gen.* **23**, 5673 (1990).
- [25] N. V. Zamfir, R. F. Casten, M. A. Caprio, C. W. Beausang, R. Krücken, J. R. Novak, J. R. Cooper, G. Cata-Danil, and C. J. Barton, *Phys. Rev. C* **60**, 054312 (1999).